

LIFE TEST OF THE SCARAB INSTRUMENT SLIPRING UNITS

J.B. Mondier^{*}, F. Sirou^{**}, P.A. Maüsli^{***}

^{*}Centre National d'Etudes Spatiales

18 avenue E. Belin, 31401 Toulouse Cedex 4, France

Telephone : 05 61 28 22 15, Fax : 05 61 28 29 85, E_mail : jean-bernard.mondier@cnes.fr

^{**}Laboratoire de Météorologie Dynamique, Ecole Polytechnique, Palaiseau, France.

^{***}Mecanex, Nyon, Switzerland.

ABSTRACT

The SCARAB instrument was designed by the Laboratoire de Météorologie Dynamique in the late 80's to study the radiation budget of the Earth from space. As part of the French-Soviet research program, the FM1 instrument was put into orbit, in February 1994, onboard a Russian platform for a 2-year mission. Unfortunately, the radiometer failed one year later. The CNES investigated the potential causes of the mission loss. This work was very difficult mainly because the onboard observable parameters were poor. However, the failure assumptions were all related to slipring units' performances. This is why a number of slipring changes were defined and implemented. A new qualification program was mandatory including vibration loads and a lifespan test. An optical head model was used in order to faithfully reproduce the flight environments and apply them to the sliprings. The life test was performed at the rated speed, that is to say a 3-year test, which included qualification margin. Meanwhile, the FM2 model was launched. It delivered only one year in-flight measurement data. The mission was stopped in April 1999 when the satellite data transmitters broke down. However, the FM2 instrument is still normally working today. The life qualification test closed up in August 2000. The results recorded during the test showed the sliprings successfully performed except for the line electrical resistance increase over life and the end of life (EOL) noise level. The hardware inspection revealed no serious damage, but a normal material wear in the sliprings and the bearings. The life test has permitted us to build an engineering database that will be at designers and users disposal for future projects using this electrical contact technology.

1. BACKGROUND

To understand how the radiation exchanges operates in our climate, in depth analysis of the earth radiation budget (ERB) needs to be carried out over a long period of time. ERB measurements have to consider three elements: first, the total incoming solar radiation, second the solar radiation that is reflected and scattered back to space at the top of the atmosphere and, finally, the thermal radiation emitted by the Earth. To obtain a global coverage with sufficient sampling, the

measurements have to be done from space. The SCANNER for Radiation Budget (SCARAB) project was initiated in 1986 as part of the French-Soviet joint project for space research. The original purpose was to provide broadband observation of the ERB and to ensure continuity of coverage after the NASA/ERBE scanner operation. The ERBE scanner on board the ERBS satellite operated successfully for over 5 years until February 1990. SCARAB-FM1, which was integrated on the Russian weather satellite Meteor-3/7, was launched almost four years later from the Plessetsk spaceport in Russia. This platform was on a circular orbit at 1200 km with an orbit inclination of 82.5°.

2. THE SCARAB INSTRUMENT

The Laboratoire de Météorologie Dynamique (LMD) developed the SCARAB instrument. It is a cross-track scanner with a spatial resolution of 60 km × 60 km. The earth-scanning angle covers 100°, which corresponds to a 1600-km swath width on the ground. The instrument consists of four telescopes (spectral channels). Two of them are broadband channels: channel #2 covers the solar reflective domain (0.2 μm to 4 μm) and channel #3 operates over the whole spectrum (0.2 μm to 50 μm). The others are narrow-band channels: channel #1 (0.5 μm to 0.7 μm) and channel #4 (10.5 μm to 12.5 μm). These are used to check that the observed scene can be identified. The ERB parameters are obtained by combining the measurements of channels #3 and #2, and the outgoing thermal radiation is computed from the difference of both measurements. The telescopes are located in a rotating, cylindrical scan head (Fig.2). The outer skin of the scan head is fitted with openings used for earth viewing and space-based calibration. The optics consists of one spherical mirror for each channel, which focuses the beam onto a pyroelectric detector (Fig.1). The radiation arriving on each detector is chopped at the pixel sampling frequency. To do this, a short-wave chopper (sw/c) covers channels #1 and #2 and a long-wave chopper (lw/c) channels #3 and #4 (Fig.2). Each chopper consists of a rotating hemispherical mirror fitted with two openings. Hence, each detector alternately receives radiation directly from outside and radiation reflected from a small reference blackbody (Fig1).

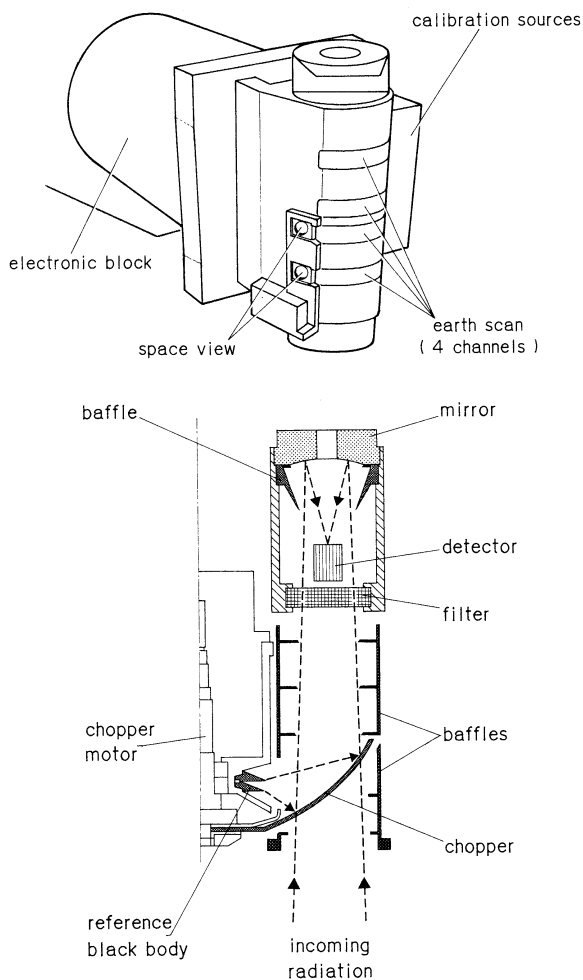


FIG. 1. Sketch of the ScaRaB instrument (upper), details of telescopes (lower).

In addition, a filters-wheel (f/wheel) is used for instrument calibration purpose. This enables four more filters to be moved in front of channels #2 and #3.

3. THE OPTICAL HEAD MECHANISMS

The optical head is a mechanical system that comprises four telescopes and the relevant data processing electronics, two choppers and one f/wheel. All the equipment is mounted on a rotating shaft, which is supported by two pairs of angular contact ball bearings (Fig.2). The choppers rotate continuously at an 8 Hz speed rate for 2 years ($500 \cdot 10^6$ cycles). The f/wheel is driven by a stepper motor associated to an 8:1-rate gear speed reducer. Compared to the choppers, this motor has to rotate far less because it is used only during the different instrument calibration modes. The entire optical head bearing lubrication is dry coated with MoS_2 -filled cages or spacers essentially to prevent optics pollution. These mechanisms are all located on a shaft, which moves in unlimited rotation. Here, two slipring units are needed to transmit the electric signals. For design reasons, they were implemented one at each end

of the main shaft (Fig.2). The resolver-side one (r/s) transfers the digitised and multiplexed measurement data as well as the f/wheel round sensor signal. With the motor-side one (m/s), the choppers angular sensor signals and the main shaft resolver signals are transferred to an outer static electronic block.

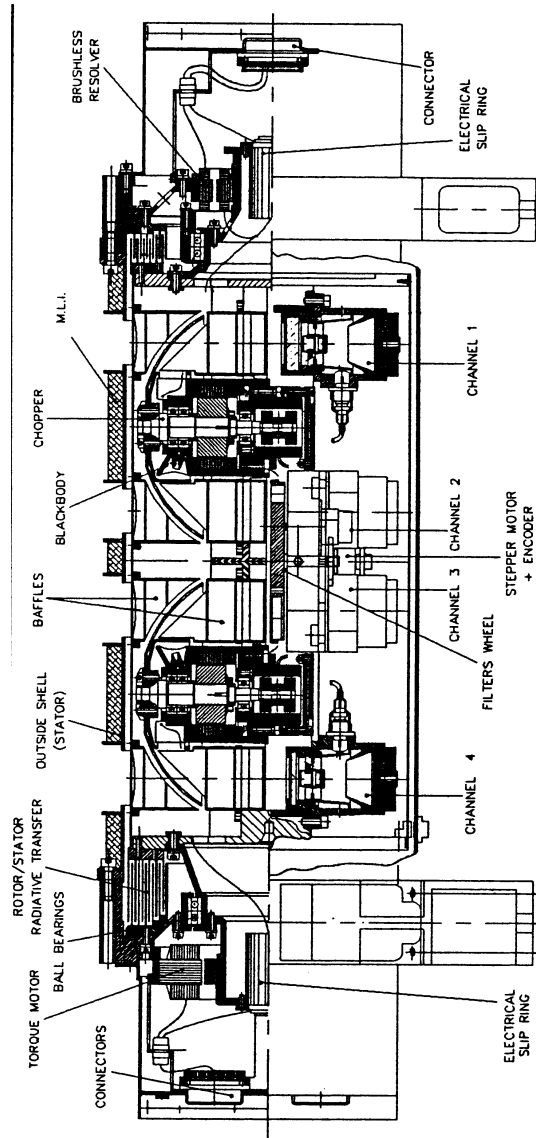


FIGURE 2 - OPTICAL HEAD DESIGN

In addition, this unit transmits the power supply of the choppers and f/wheel motors. Each unit comprises 36 tracks rated at 500 mA. The maximum current value encountered in flight is 100 mA. The sliprings consist of gold alloy solid rings and single wire brushes. The slipring rotor rotating guidance is provided by a couple of MoS_2 -lubricated bearings. The slipring units were manufactured and supplied by MECANEX.

4. SCARAB FM1 FLIGHT

SCARAB FM1 provided good ERB in-flight data from 24 February 1994 to 6 March 1995. Then, unexpectedly, the instrument switched over to the rest mode and remained shut off. The root reason for this behaviour

has still not been explained, but it might be related to an electrical power defect somewhere in the optical head. When the instrument restarted, the thermal transient environment observed near the lw/chopper was probably the cause of the detected failures in the lw/c velocity control. This might have been a thermo-mechanical problem that ended when the temperature returned to its nominal value, several hours later. Further, the channels scientific data examination has shown that the scan head stopped rotating or was submitted to low level oscillations. For two months, several scan motion restarts were attempted by commanding both different instrument modes and on/off sequences. We waited several hours between each command to let the optical head cool itself down and thus create thermal effects. All of this provided no positive results on the scan body that remained stationary. But it showed that the electronic sequencer was not responsible for the failure. Meanwhile, other troubles appeared on the f/wheel. Several offsets were observed with the stepper motor between the commanded positions and the ones really reached. These defects lasted several days and eventually got worse. As a result, a f/wheel uncontrolled motion caused an ever lasting f/wheel mode probably because the round reset sensor was never passed over. Finally, the instrument was switched off on 5 May 1995.

5. FAILURE ANALYSIS

The poor number of observable parameters made the breakdown particularly difficult to understand. Only science data telemetry, blackbody temperatures and motion control errors of scan, choppers and f/wheel were available. Based on this information, optical head behaviour analysis during the failure phase was carried out. As a result, no single point failure could explain all the observed successive problems. However, it was determined that all the identified defects after the instrument restart were related to a slirings function. Moreover, only the motor-side slirring unit was involved in the problems that occurred. The signals going through the resolver-side slirring unit were not affected by any failure. Also, the investigations recalled a track pollution that occurred on a slirring unit during ground tests. This pollution was caused by TiC particles released by the bearing balls. It created an electrical insulation over several tracks that affected the f/wheel stepper motor power lines. When the motor windings were supplied, inductance effects produced high voltage in the lines. In the slirings, gold wear particles aligned themselves along the magnetic field lines. This created a parasite circuit between the tracks that were able to generate short-circuits.

Although no evidence could clearly show the slirings exclusive involvement in the flight breakdown, this device was somehow related to the mission loss. Therefore, a mechanical failure study of the slirings was carried out to improve the FM2 units' capacity.

6. SLIRINGS UNIT RE-DESIGN

The FM1 slirring units had been selected as on the shelf components not designed for a space application. The device analysis focused on the bearings and the slirings. The FM1 rotor guidance configuration consisted of two bearings of different sizes. Stress analysis showed that the vibration loads applied to the unit were likely to over-stress the smaller bearing, and not the larger one. This is why a new configuration was adopted with two identical bearings. Another problem we faced was the bearing preload. In the FM1 design, a screw acting directly on the small bearing inner race (O mounting) gave a solid preload. As a result, the unit could tolerate no thermal expansion. Moreover, the preload value could not be accurately controlled at integration level. Thus, it was decided to set a soft preload obtained by elastic washer deflection. So, the bearing preload value was adjustable and could be checked on every flight model. The last bearing change regarded the lubrication. On the FM1, the lubrication solution was based on both TiC-coated balls and an MoS₂ spray deposit, which is not qualified for space use. This process could not guarantee either the lubricant amount control or whether it would remain in the bearings. This is why a PVD MoS₂ coating on the tracks was chosen for FM2. A Duroid 5813 cage replaced the FM1 bearing metallic cage and flanges were added to each FM2 bearing to prevent wear particles from migrating towards the electrical tracks.

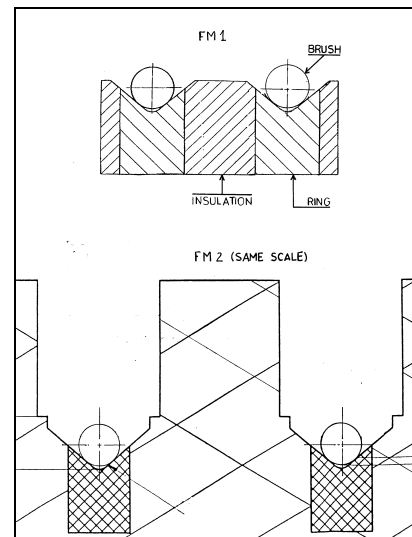


Figure 3 – Shape evolution between FM1 and FM2 slirings

One main point was analysed on the slirings: the insulation gap between the tracks. Figure 3 shows a cross section of the slirings pattern. From FM1 to FM2, the only change was the insulation material shape between the rings. The reason for this was to increase the gap between two adjacent tracks as much as possible, and still meet the size requirement. The same FM1 materials were used for FM2.

7. RE-QUALIFICATION PROGRAM

All the changes done on the sliprings were considered as critical regarding the qualification status. A complementary test was necessary to validate the definition changes and show the FM2 flight reliability. To do this, it was decided to use a qualification model (QM) of the optical head fitted with the following parts: the main bearings, the motor and the relevant resolver sensor, two sliprings units and dummy masses for all the other parts born by the rotating head (choppers and f/wheel). Thus, the QM used was representative of flight definition for masses and moments of inertia. This was essential to obtain realistic equipment behaviour in response to the vibration loads. The flight thermal environment measured on FM1 was not considered as critical for the sliprings. So, thermal vacuum cycling was not included in the test sequence. The main part of the FM2 qualification was the life duration ground test, which took place in the CNES mechanism laboratory. It was performed under ultra-vacuum at the rated speed in order to respect the tribological operating conditions in the sliprings contacts. An electronic block identical to the FM2 one controlled the scan motion. All the instrument running modes (measurement and calibrations) were sequentially executed according to the most demanding mission pattern, that is to say the slipring capabilities. The consequence of the rated velocity choice was to perform a 3-year test to meet the 2-year mission requirement. From the test start up, in mid-August 1997, it was quite clear that the life span might end after the FM2 launch. However, doing it would give pre-flight interesting equipment health status. Eventually, the FM2 instrument was launched from the Baikonour spaceport on 18 July 1998 on the Russian weather satellite Resurs1/4. Unfortunately, the failure of the satellite second data transmitter occurred on 7 April 1999, prematurely ending the SCARAB mission. Afterwards, the servicing telemetry showed that the instrument kept on working normally. Nevertheless, the slipring units' life qualification test continued right to the end in August 2000. The new test objective was to provide engineering data for a flight on board the new Megha Tropiques satellite project.

8. TEST CONFIGURATION

The following table summarises the main test requirements to be met by the sliprings units.

Electrical specifications	
Nominal current	100 mA
Line resistance (including 400 mm wire)	$\leq 0,5 \Omega$
Line resistance noise 0-peak	$\leq 40 \text{ m}\Omega$
Line resistance variation over life span	$\leq 70 \text{ m}\Omega$
Insulation resistance between tracks	$\geq 100 \text{ M}\Omega$

Mechanical specifications	
Number of in-flight rotations with margin	15 millions
Friction torque under vacuum	$\leq 75 \text{ cN.cm}$
Starting torque under vacuum	$\leq 150 \text{ cN.cm}$
Environment	
ambient temperature	$+5^\circ\text{C} \leq \theta \leq +35^\circ\text{C}$
Ultra-vacuum chamber	$\leq 10^{-7} \text{ mbar}$

The qualification test goal was to demonstrate that the electrical sliprings end-of-life performances could satisfy the specifications. The FM2 flight clearance status was dependent on test data. So, it was vital to note the units' performances continuously throughout the test. This is why all the electrical measurements were monitored and recorded daily. The slipring units' qualification could not be performed for each single track. To minimise the test bench complexity, several tracks were then serially connected to create independent electrical resistive circuits that could be power supplied and measured from the outside of the vacuum chamber. Two groups of tracks were built like this for each slipring unit. A controlled 100-mA constant current supplied each circuit throughout the life test. The overall drop voltage was measured for each circuit. Some other tracks were selected from each unit for electrical insulation test. Six independent slipring sectors were distributed over the two units. For each sector, the even tracks were connected together and, the same thing was done with the odd tracks. The insulation impedance was measured between the two track series with a mega-ohmmeter. The slipring remaining tracks were reserved for the f/wheel motor power supply transfer and the winding excitation current transmission of the scan resolver. The performance of these tracks could not be directly measured. We observed how functions (f/wheel motor, scan motion) which were related to the tracks reacted. The following table summarises the slipring tracks allocation.

Test bench channel #	Slipring track #	Qualification purpose
Motor-side slipring unit		
5	1 to 4	Insulation
6	5 to 9	Insulation
1	10 to 17	Drop voltage
No measure	18 to 21	F/wheel motor supply
No measure	22 and 26	Resolver winding
No measure	23 to 31	F/wheel motor supply
2	32 to 35	Drop voltage
No measure	36	Ground continuity

Resolver-side slipping unit		
3	1 to 6	Drop voltage
7	7 to 12	Insulation
8	13 to 18	Insulation
9	19 to 24	Insulation
4	25 to 30	Drop voltage
10	31 to 36	Insulation

9. TEST RESULTS

Vacuum chamber pressure

The vacuum chamber used for the life test is equipped with an ionic-pumping system. This allows a very low residual pressure level, which is frequently required for vacuum tested mechanisms, especially for tribological purpose. In our test, the chamber vacuum pressure was at 5×10^{-6} mbar at start up, in mid-August 1997. This value reached 10^{-7} mbar less than one month later. Afterwards, it took five months for the pumping device to bring the pressure down to 6×10^{-9} mbar, because of the mechanism material outgassing that is always predominant in the beginning of life testing. Moreover, this was accentuated by the thermal dissipation from the sliprings, wires and motor windings ohmic losses. The chamber pressure fluctuated around 6×10^{-9} mbar until the end of the test.

Drop voltage measurements

The four slipping tracks-groups used for the electrical contact resistance test did not show the same features throughout their lifespan, especially regarding electrical noise. However, all the groups provided a similar behaviour pattern. This is why the results of only one tracks-group (test bench channel #1) is presented below. In the following diagrams, the contact electrical resistance has been plotted according to the following main assumptions:

- the unit wire impedance is constant throughout the test and is subtracted from the overall drop voltage,
- the total 8-track group impedance (electrical contacts) is equally shared between the tracks.

Thus, the drop voltage measurements were used to make single-track impedance diagrams. Each diagram comprises four curves. The daily measurement data was processed to obtain the min, max, mean and standard deviation values. The last one represents the impedance noise level.

Figure 4 shows two separate phases. The first one covers the first couple of months of the test. At start up, the mean impedance value stood up at 15 mΩ, and the impedance noise was about 1 mΩ. After this very quiet phase, some interference appeared in the contacts and remained for more than one month, as the max and the noise curves attest. A great amount of wear particles may have been generated within a short period of time. This probably created difficult brush sliding conditions.

Disturbances may have disappeared when the early wear particles were removed from the tracks or began to collect on the brush. This phenomenon could be considered as a run-in process. During this phase, the mean impedance remained relatively low at 40 mΩ. The disturbances exhibited high values but in a limited number of occurrence.

The second phase spread over almost two years. During this period, the sliding contacts cumulated nearly 10 millions turns. Their electrical performance was relatively stable, revealing healthy sliprings. The mean impedance value oscillated at around 50 mΩ, and the noise level remained below 40 mΩ. At this point of the test (mission completion), the electrical performance still met the requirements.

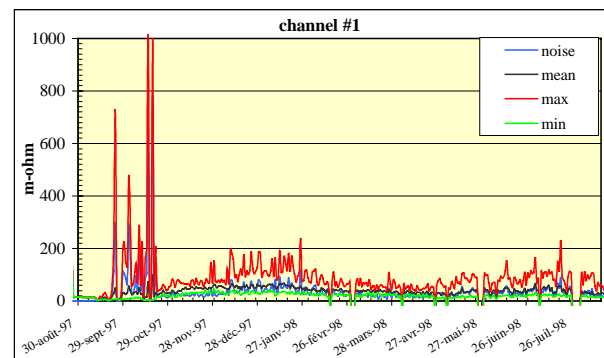


Figure 4 – one-track impedance – test first year

A significant change in behaviour can be seen in figure 5, which shows the last year of the test. The contact sliding distance of that period of time is equivalent to 5 million turns. In mid-1999, the mean impedance had risen up to 180 mΩ. At that time, the noise level had slightly increased to roughly 60 mΩ. Then, in mid-October 1999, the max values suddenly increased, revealing new interference in the brush-track contacts. These degraded sliding conditions remained until the end of the test. Nevertheless, the mean impedance stopped increasing at 220 mΩ, by the end of 1999 and even decreased steadily for the last six months of the life test. The electrical noise closely followed the same evolution. In addition, the min values were very similar to the mean ones. This indicates that a relatively poor number of high values were part of the measurement sampling. The presence of wear particles in the contact may have been responsible for the contact impedance degradation, as the sliprings had not yet been worn out. The final values of the test are 180 mΩ for the mean impedance and 150 mΩ for the noise level. The mean impedance was multiplied by 5 since the beginning of the test. A noise level of 22% 0-peak of the total 8-track group impedance was noted.

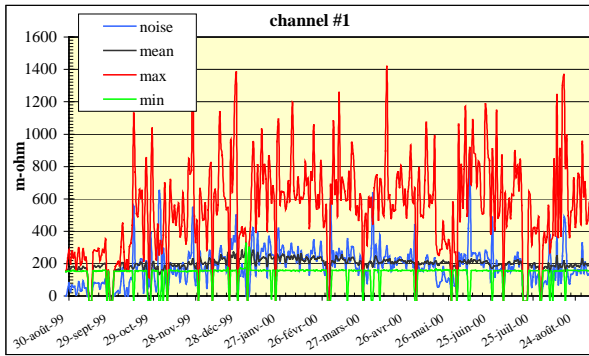


Figure 5 – one-track impedance -test last year

Examining the tested tracks' results, one interesting feature was identified. The sliding distance does not systematically affect the contact impedance degradation. In fact, the contact disturbance slump may even occur far from the run-in phase.

Insulation measurements

Six measurement channels were used to test insulation. All of them provided the result $\infty\Omega$ throughout the lifespan, that is to say a perfect electrical insulation under the test conditions.

Electrical performances balance

The following table summarises the EOL electrical test results, given for a single track.

Electrical specification	Motor-side sliping unit		Resolver-side sliping unit	
	1	2	3	4
Bench channel number	1	2	3	4
①Line resistance (m Ω) specif. $\leq 0,5 \Omega$	268	325	296	263
②Line resistance noise 0-peak (m Ω) specif. $\leq 40 \text{ m}\Omega$	150	50	163	20
③Line resistance variation over life span specif. $\leq 70 \text{ m}\Omega$	180	238	208	175
Bench channel number	5 and 6		7 to 10	
④Insulation resistance between tracks (M Ω) specif. $\geq 100 \text{ M}\Omega$	$\geq 10^6$		$\geq 10^6$	

Line resistance and the line resistance life variation are globally homogeneous. Thus, we can say that, under our test conditions, this sliping technology provides a relatively good reproducible rate of electrical contact impedance over the tracks. This is even more remarkable for performance ③ where the evolution through life depends on wear. On the other hand, the electric noise proved to be different for each track. This could be the result of preload scattering among the brushes. Hardware inspection has provided more information on this point - as the brush preload is also related to the material wear (see § 10).

As far as the mission requirements are concerned, the final results show that only specification ① has been met. The qualification life test is not conclusive for impedance life increase and electrical noise level. It seems that the requirements ② and ③ are too demanding for this sliping technology. Whereas performance ④ easily met the requirement.

Friction torque evolution

The supplier measured the units' dynamic friction torque during the reception tests. After the life test, a new measurement was done at CNES, in the same ambient conditions. The following table summarises the results.

Torque measured at 3 rpm (cN.cm)	Motor-side sliping unit	Resolver-side sliping unit
during reception	4	4
After life test	30	42

The measurements did not show how the torque was distributed between the bearings and the sliprings. However, the sliping may cause the main part of this torque. Although the life amplification factor is close to 8 or 10 for each sliping unit, the final torque level remains below the requirement of 75 cN.cm. This is of no real concern since the sliping hardly contributes to the overall scan torque budget.

Life test conclusions

Throughout the life test, the optical head operated nominally. The scan motion controlled by the main shaft resolver experienced no position error. Likewise, the f/wheel stepper motor operated without failure. Thus, each function that depended on sliping current transmission operated correctly.

Several sliping lines were directly tested. The EOL line resistance met the requirement and was relatively homogeneous over the measured tracks. On the other hand, the average value of the line resistance increase over life was three times worse than that stipulated in the specification. We conclude that this requirement is obviously too demanding for the chosen technology and for such a long lifespan. In addition, the test clearly showed that the electrical noise results varied enormously over the four groups of tracks. The impedance noise value ranged from 4% to 26% of the mean impedance. However, we would like to point out that in spite of statistical evidence, the instrument optical head performed well throughout the test. It would be interesting to look into the real needs regarding the values that do not meet the specification. Lastly, all the insulation measurements were successful.

Since the end of the SCARAB FM2 instrument mission, the sliping units' qualification is no longer a concern regarding the SCARAB project. However, these aspects will have to be discussed for a possible re-use of the instrument in the Megha Tropiques mission.

10. HARDWARE INSPECTION

After the qualification life test, the two slipping-units were dismantled from the equipment. One was sent back to the supplier MECANEX and the other one stayed at CNES. Both were subjected to a detailed inspection. Figure 6 shows an overview of the unit inspected at CNES.

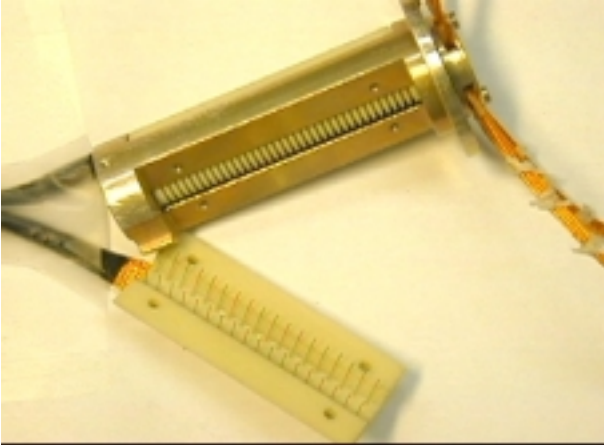


Figure 6 – overview of one slipping unit

The light coloured part is one of the two brush-supports. It is removed from the slipping housing. No apparent damage could be seen on the brushes. A large number of tiny golden particles were observable on the support surface. The shaft and the tracks are partially visible through a housing aperture. By naked eye observation, it was not possible to identify any track unexpected wear or any insulation defect.

On figure 7, we can see two brushes from the same brush support. On the right side, the brush exhibits a large contact area. This area is located just before the brush bent end. This particular shape is designed for brush mounting easiness. The contact curved shape is the result of brush friction on the track. Inside the contact zone, sliding lines have been grooved along the motion direction. At contact outlet, accumulated wear particles remain glued onto the brush. This is even more visible on figure 8.

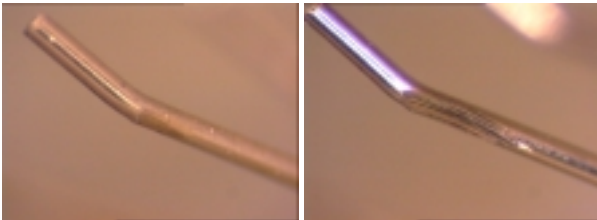


Figure 7 – brush contact area

On the left side of figure 7, almost the same can be observed. However, a difference is the contact area size. This brush is obviously less used than the other one. This could be the result of a lower preload. Among all the brushes, the inspection revealed a very scattered wear rate. The above right side brush is one of the most

worn brushes. In this case, the material removed volume is less than the third of the original size.

Obtained by SEM analysis, figure 8 shows the material shifting inside the contact area as well as the friction lines. The brushes are coated with tiny metallic debris of typically a few microns size. The brush contact surface X-analysis revealed that the track material was present. A part of the wear particles from both track and brush has collected onto the brush.

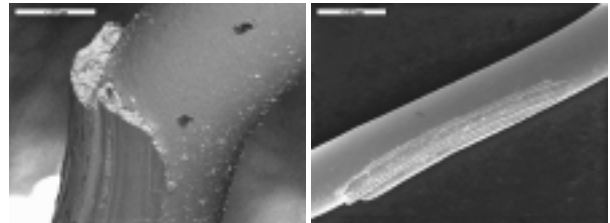


Figure 8 – brush SEM viewing

Troughout lifespan, some gold alloy was removed from the track and gathered by the brushes. The picture also shows the typical shape difference between the inlet and the outlet contact area.

Figure 9 shows a typical track EOL shape by SEM viewing. On the left side, the track is side viewed. The light part of the picture represents the metallic ring and the dark one is the inter-ring insulation. The sliding track is the worn part of the ring located in the center of the picture. The brush shape has been grooved at the bottom of the track. Very little metallic debris of typically a few microns size was found all over the ring.

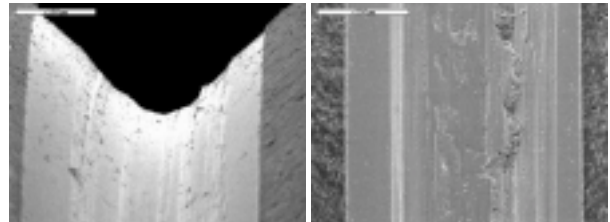


Figure 9 – typical track pictures

On the right side, the track is front viewed. At the bottom of the track, wear particles have been laminated between the brush and the track, and even pushed away from the track. The tracks do not seem to be excessively worn out regarding the large number of performed rotations. Among the rings observed, no bearing particles could be found. This means that bearing flange confined the wear particles throughout the test.

Figure 10 shows the pictures of the inner and outer race of one unit bearing.

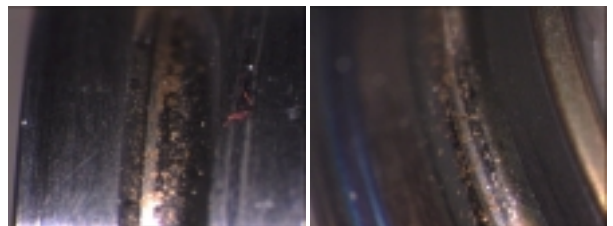


Figure 10 – bearing inner and outer race

On the left side, in the center, we can see the rolling track of the inner race. The black part represents the M_oS_2 coating. X-analysis showed that this coating is in the same state as it was at the origine. It has only been partially removed from the track, leaving a white narrow stripe that is located on the ball rolling path. We can notice that a large number of golden particles are spreaded all over the track. These particles have been flattened out by the balls and now remain glued on the track. All this golden debris certainly came from the slipping part of the unit. This did not prevent the bearing from working well. The same inner race observations are valid for the outer race, which is displayed on the right side of figure 10.

Figure 11 shows a more detailed view of the bearing inner race obtained by SEM analysis. The ball rolling path is not visible. This means that no direct ball to race steel interaction was experienced during the test. The bearing EOL capacity is still not reached.

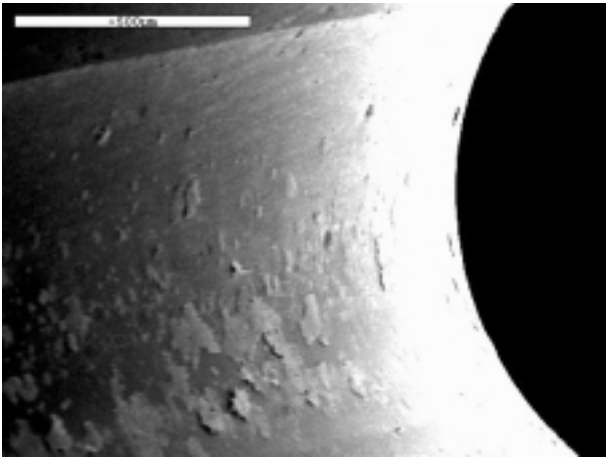


Figure 11 – bearing inner race

Figure 12 shows on the left side a Duroïd 5813 cage alveole and, on the right side, one typical bearing ball. We can notice that the ball left marks on the cage alveole. These ones are located in the middle of the cage thickness. Again, golden debris were trapped between the ball and its alveole. The cage wear rate seems very poor. This may be related to the moderate designed bearing preload.

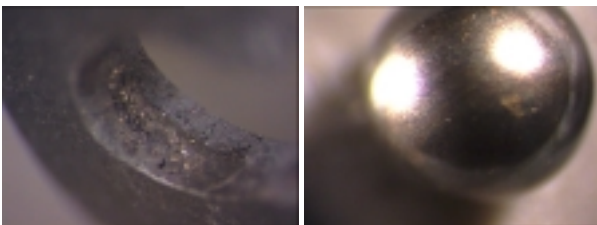


Figure 12 – bearing cage and ball

A thin M_oS_2 film coats all the bearing balls. As the balls were not initially coated, this could be essentially caused by the race M_oS_2 removal. Any marks could not be found on the balls.

11. CONCLUSIONS

The CNES worked on the SCARAB FM1 instrument mission failure analysis. As part of the FM2 instrument modification program, the CNES mechanism department helped to re-design the instrument slipping unit and carried out a new life test to qualify the design changes. The test was performed at the rated speed and lasted three years. The results showed that this kind of slipping, based on gold contact technology, meets long-term life requirement (15 millions turns) at an average speed of 10 rpm for the transmission of a 100-mA current. In addition, electrical performances tested showed that this technology should be used according to its contact tribological nature. This is to say the line resistance stability requirement must not be too demanding if the line resistance level is not critical. Also, thanks to this test, the CNES was able to build a detailed engineering database that could be useful, in the future, for designers and users of this kind of device.

One slipping unit was dismantled and inspected in details at CNES after the lifespan test. The slipping wear rate was analysed by optical and SEM means. As a result, the brush wear rate is relatively scattered and globally not critical regarding the mission life. A poor wear rate was also found in the tracks. A large amount of tiny golden particles covers almost all the parts surface. The bearing inspection showed a safe EOL wear state. The solid lubricant transfer operated well between the tracks and the balls. It was less efficient between the cage and the balls, according to the poor wear rate of the cage.